NUKLEONIKA 2000;45(4):235–241

ORIGINAL PAPER

Measurement of liquid holdup and axial dispersion in trickle bed reactors using radiotracer technique

Harish Jagat Pant,
Anil Kumar Saroha,
Krishna Deo Prasad Nigam

Abstract The holdup and axial dispersion of aqueous phase has been measured in trickle bed reactors as a function of liquid and gas flow rates using radioisotope tracer technique. Experiments were carried out in a glass column of inner diameter of 15.2×10^{-2} m column for air-water system using three different types of packings i.e. non-porous glass beads, porous catalysts of tablet and extrudate shape. The range of liquid and gas flow rates used were 8.3×10^{-5}–3.3×10^{-4} m^3/s and 0–6.67×10^{-4} m^3/s, respectively. Residence time distributions of liquid phase were measured and mean residence times were determined. The values of liquid holdup were calculated from the measured mean residence times. It was observed that the liquid holdup increases with increase in liquid flow rates and was independent of increase in gas flow rates used in the study. Two-parameter axial dispersion model was used to simulate measured residence time distribution data and values of mean residence time and Peclet number were obtained. It was observed that the values of Peclet number increases with increase in liquid flow rate for glass beads and tablets and remains almost constant for extrudates. The values of mean residence time obtained from model simulation were found to be in good agreement with the values measured experimentally.

Key words axial dispersion model • holdup • mean residence time • Peclet number • residence time distribution • trickle bed reactor

H. J. Pant✉
Isotope Applications Division,
Bhabha Atomic Research Centre,
Trombay, Mumbai 400 085, India,
Fax: 91-22/ 5505151, 5519613,
e-mail: hjpant@apsara.barc.ernet.in

A. K. Saroha
Department of Chemical Engineering,
Thapar Institute of Chemical Engineering and Technology,
Patiala 144001, India

K. D. P. Nigam
Department of Chemical Engineering,
Indian Institute of Technology,
Hauz Khas, New Delhi 110 016, India

Received: 29 February 2000, Accepted: 14 July 2000

Introduction

Trickle bed reactor (TBR) implies a reactor in which a liquid phase and a gas phase flow cocurrently downward through a fixed bed of catalyst particles while the reaction takes place. In certain cases the two phases also flow cocurrently upward. The cocurrent upward flow operation provides better radial and axial mixing than the downward flow operation due to which the heat transfer between the liquid and solid phases is better. This is useful in highly exothermic reactions in which products needs to be removed from the reactor continuously. However due to higher axial mixing in the upward flow operation, the degree of conversion, which is a crucial factor in the operation of a reactor, is low. Therefore, cocurrent downward operation is preferred due to better mechanical stability, lower axial mixing and less flooding, thus facilitating processing of higher flow rates and increased reactor capacity.

In the last few decades the TBRs have been studied extensively by chemical engineers due to their suitability for many operations in petroleum refining, chemical, petro-chemical and bio-chemical processes. The major processes carried out in TBRs are hydrotreating, hydrocracking, hydrodesulfurization, hydrodenitrogenation, hydrodewaxing, hydrodemetallisation and hydrofinishing. In effluent treatment plants, the trickle bed reactors are used for removal of organic matter from

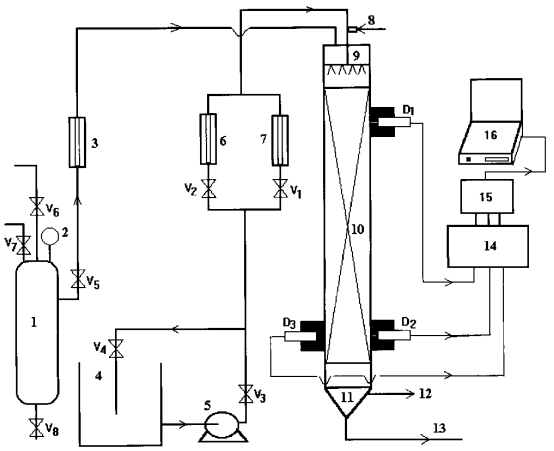

Fig. 1. Schematic diagram of experimental setup. 1 – surge tank, 2 – pressure gauge, 3 – air rotameter, 4 – water tank, 5 – liquid feed pump, 6-7 – liquid rotameters, 8 – tracer injection port, 9 – liquid distributor, 10 – trickle bed reactor, 11 – gas-liquid separator, 12 – air outlet, 13 – liquid outlet, 14 – counter, 15 – data acquisition system, 16 – laptop computer; D_1, D_2, D_3 – collimated radiation detectors; V1...V8 – valves.

wastewater streams by aerobic bacterial action. The potential applications, advantages and disadvantages of the TBRs have been reviewed in two recent articles [3, 8].

The knowledge of mean residence time, holdup and axial dispersion is a basic requirement to evaluate the reactor performance, its optimal size, the physical and chemical interactions and the pumping requirements. Liquid holdup and axial dispersion are two key parameters to describe the performance of a TBR. Residence time distribution (RTD) analysis facilitates the determination of these parameters. Radiotracer techniques are widely used to measure RTD of process material in industrial process systems because of their various advantages over conventional tracer techniques [8]. This paper describes measurement of RTD, determination of mean residence time (MRT), holdup and axial dispersion of aqueous phase using radiotracer technique.

Experimental

The schematic diagram of the experimental setup is shown in Fig. 1. A series of radiotracer experiments was performed to measure the RTD of liquid phase in a glass column of 15.2×10^{-2} m inner diameter. The experiments were carried out with three different types of packings i.e. non-porous glass beads, porous catalysts of tablet and extrudate shape with air-water flow at ambient conditions. The air (density: 1.293 kg/m^3, viscosity: 1.83×10^{-5} Pa.s) and water (density: 997.0 kg/m^3, viscosity: 18.2×10^{-5} Pa.s) flowed cocurrently downward through the column which had a packed height of 1.25 m. Table 1 lists the details of the packings and range of Reynolds number used. The liquid stored in a tank of 0.2 m^3 capacity was continuously pumped into the column from the top through a distributor mounted 0.1 m above the packing. The liquid distributor consists of a stainless steel tube of diameter 6.4×10^{-3} m to which tubes of diameter of 3.2×10^{-3} m were attached. There were 37 holes of the size of 1.5×10^{-3} m arranged in a square pitch of 2.0×10^{-2} m [9]. The air was continuously introduced into the column from the top from a compressor after passing through an air saturator (surge tank). After passing through the packed bed, the liquid and gas phases were separated in a gas-liquid separator at the bottom of the column. Two precisely calibrated rotameters were used to measure the liquid and gas flow rates. The air was allowed to escape into the atmosphere while the water was discharged into a drainage pipeline. ^{99m}Tc (half life: 6 h and gamma energy 0.14 MeV (91%)) as sodium pertechnatate was used as a tracer. ^{99m}Tc was extracted from a ^{99}Mo/^{99m}Tc-generator and about 10–20 MBq activity was used in each run. The experiments were performed at different combinations of gas and liquid flow rates. The tracer was injected instantaneously into the inlet feed line through an injection port at the top of the column using a calibrated glass syringe. The tracer was injected after achieving steady state flow. The tracer movement was monitored at the inlet (D_1) and outlet (D_2) of the column using collimated NaI(Tl) scintillation detectors (M/s Bicron Corporation, U.S.A.) separated by a distance of 1.25 m. In order to investigate the radial distribution of liquid, an additional detector D_3 was also mounted diametrically opposite to detector D_2 at the reactor outlet. The detectors were connected to a multichannel data acquisition system (DAS) supplied by M/s Electronic Enterprises Pvt. Ltd., Mumbai, India. The DAS was set to record 1000 data points at an interval of 0.2 seconds. In the initial few experiments with glass beads as packing material, the interval was kept 0.5 seconds. The tracer concentration was recorded until the radiation level at the outlet comes to the background level. The recorded data was transferred to the computer for subsequent analysis.

Data analysis

Determination of mean residence time and holdup

The data recorded were treated and analysed using a Residence Time Distribution analysis software provided by the International Atomic Energy Agency Vienna, Austria [7]. The data treatment includes background subtraction, zero shifting and tail correction. Figs. 2a, 2b and 2c show three typical treated normalised residence time distribution curves.

Type of packing	*Particle diameter, d_p (m)	Bed voidage (ε)	Reynold No. for liquid (Re_L)	Reynold No. for gas (Re_G)
Glass beads	4.45×10^{-3}	0.38	23–90	0–12
Tablets	4.62×10^{-3}	0.36	24–98	0–12
Extrudates	4.8×10^{-3}	0.36	25–102	0–13

Table 1. Details of the packings used.

* Particle diameter is defined as the diameter of a sphere of the same volume as a particle.

$$Re = \frac{d_p q u}{\mu}$$

where: q – density (kg/m^3), u – superfinal velocity (m/s), μ – viscosity (Pa.s)

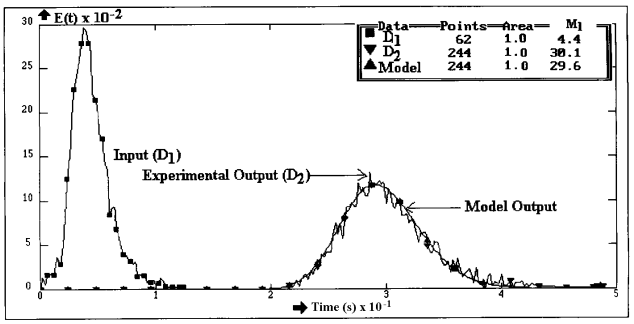

Fig. 2a. Comparison of experimental and model simulated RTD curves. (Packing: glass beads, $Q_g = 5.0\times10^{-4}$ m^3/s, $Q_l = 2.5\times10^{-4}$ m^3/s, Pe = 150, ADE = 0.00257).

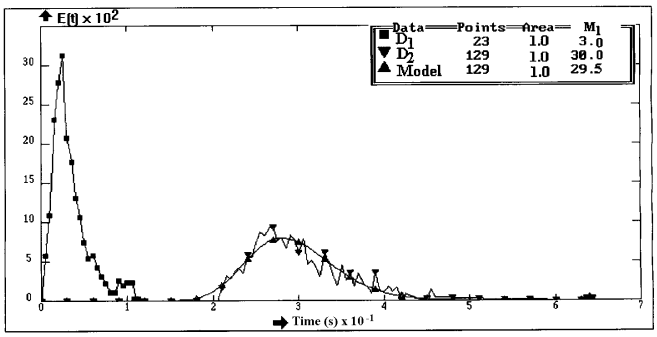

Fig. 2b. Comparison of experimental and model simulated RTD curves. (Packing: tablets, $Q_g = 5.0\times10^{-4}$ m^3/s, $Q_l = 2.5\times10^{-4}$ m^3/s, Pe = 65, ADE = 0.00388).

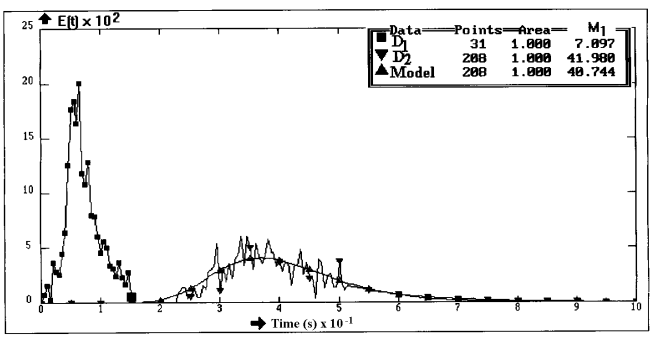

Fig. 2c. Comparison of experimental and model simulated RTD curves. (Packing: extrudates, $Q_g = 0.0$ m^3/s, $Q_l = 0.83\times10^{-4}$ m^3/s, Pe = 30, ADE = 0.00281).

First moments (M_i) of the input and the output tracer concentration curves were determined using the following relation [8]:

$$(1)\qquad M_i = \frac{\int_0^t t_i C_i(t_i)dt}{\int_0^t C_i(t_i)dt}$$

where i = 1 for input curve, i = 2 for output curve.
The difference of first moments of the two curves gives MRT of process material in the system. Thus:

$$(2)\qquad \bar{t}(\mathrm{MRT}) = M_2 - M_1$$

where, M_1 and M_2 are values of the first moments of input and the output curves, respectively. The theoretical MRT (τ) of the material in a closed system is given as:

$$(3)\qquad \tau = \frac{V}{Q}$$

where: V – volume and Q – flow rate. For a normally operating closed system the theoretical and the experimentally measured MRT should be the same. Based on the calculated MRT, the liquid holdup was calculated using the following relation:

$$(4)\qquad H_T = \frac{\bar{t}\,Q_L}{V_R}$$

where: H_T – liquid holdup, $\bar{t}$ – experimentally determined MRT, Q_L – volumeteric liquid flowrate, V_R – effective reactor volume. The values of MRT and liquid holdup at different operating conditions used are given in Tables 2, 3 and 4 for glass beads, tablets and extrudates, respectively.

Residence time distribution and model simulation

The residence time distribution (RTD) is a characteristic function of continuous process systems and provides information on malfunction(s), if any, and flow pattern i.e. degree of mixing. The RTD is defined as a normalised response of the system to an ideal impulse injection of stimulant in the form of δ-Dirac distribution [1]. If an ideal impulse of tracer is injected at the inlet of the system at time t=0 and its concentration is measured as a function of time at the outlet, then E(t)dt represents the fraction of the tracer having residence time between time interval (t, t+dt) or as otherwise stated the probability for a tracer element to have a residence time between interval (t, t+dt).

$$(5)\qquad E_i(t) = \frac{c_i(t)}{\int_0^\infty c_i(t)dt}$$

such that:

$$(6)\qquad \int_0^\infty E_i(t)dt = 1$$

where: i = 1,2…..n, $c_i(t)$ – tracer concentration and $E_i(t)$ – residence time distribution function.

The industrial TBRs are operated either in the transition region from trickle to pulse flow regime or in pulse flow regime. As described earlier a TBR is one in which liquid and gas phases flow cocurrently downward through a fixed bed of catalyst particles. Ideally, the flow should be plug flow but some axial intermixing is always inevitable. The residence time of tracer in the column is small as compared to the time required for tracer to diffuse into the catalyst pores. Therefore, it is assumed that the porosity of catalyst has a negligible affect on the tracer movement in the column. Based on the above considerations, the obtained RTD data were simulated using a two-parameter axial dispersion model (ADM) with open-open boundary conditions. The one-dimensional differential equation of ADM for fluid flow is given as [2, 5]

Table 2. Holdup and Peclet number for glass beads.

Run No.	Q_g (m^3/s)	Q_1 (m^3/s)	$\bar{t}$(s)	H_T	$\bar{t}_m$ (s)	Pe	1/n Σ|Y(t)−Y_m(t)|
1	0	8.3×10^{-5}	31.0	0.30	30.0	47	0.00261
2	0	1.67×10^{-4}	22.0	0.40	21.0	84	0.00300
3	0	2.5×10^{-4}	25.5	0.74	25.0	98	0.00323
4	0	3.17×10^{-3}	20.0	0.74	20.0	88	0.00400
5	1.67×10^{-4}	1.0×10^{-4}	29.0	0.33	27.5	60	0.00178
6	1.67×10^{-4}	1.5×10^{-4}	47.0	0.82	46.0	72	0.00105
7	1.67×10^{-4}	2.5×10^{-4}	23.0	0.66	22.0	86	0.00353
8	1.67×10^{-4}	2.8×10^{-4}	20.0	0.67	20.0	84	0.00341
9	1.67×10^{-4}	3.17×10^{-3}	21.0	0.79	21.0	115	0.00334
10	3.3×10^{-4}	1.0×10^{-4}	34.5	0.40	33.5	52	0.00270
11	3.3×10^{-4}	1.5×10^{-4}	34.0	0.60	33.0	54	0.00360
12	3.3×10^{-4}	1.83×10^{-4}	32.0	0.68	31.5	58	0.00340
13	3.3×10^{-4}	2.5×10^{-4}	25.0	0.72	24.0	70	0.00397
14	3.3×10^{-4}	2.8×10^{-4}	20.0	0.75	20.0	76	0.00635
15	3.3×10^{-4}	3.17×10^{-3}	20.0	0.77	21.0	207	0.00427
16	5.0×10^{-4}	8.3×10^{-5}	32.0	0.30	32.0	65	0.00268
17	5.0×10^{-4}	1.67×10^{-4}	36.0	0.69	35.0	105	0.00190
18	5.0×10^{-4}	2.5×10^{-4}	26.0	0.75	25.0	150	0.00257
19	5.0×10^{-4}	3.17×10^{-3}	21.0	0.77	20.5	160	0.00400
20	6.67×10^{-4}	8.3×10^{-5}	31.0	0.30	29.0	48	0.00243
21	6.67×10^{-4}	1.67×10^{-4}	36.0	0.70	36.0	104	0.00179
22	6.67×10^{-4}	2.5×10^{-4}	26.0	0.74	25.0	124	0.00258
23	6.67×10^{-4}	3.17×10^{-3}	21.0	0.77	21.0	206	0.00270

Table 3. Holdup and Peclet number for tablets.

Run No.	Q_g (m^3/s)	Q_1 (m^3/s)	$\bar{t}$ (s)	H_T	$\bar{t}_m$ (s)	Pe	1/n Σ|Y(t)−Y_m(t)|
1	0	8.3×10^{-5}	42.0	0.43	38.0	28	0.00467
2	0	1.67×10^{-4}	24.0	0.50	23.5	51	0.00614
3	0	2.5×10^{-4}	25.0	0.77	23.0	66	0.00599
4	0	3.3×10^{-4}	22.0	0.90	21.0	44	0.00334
5	1.67×10^{-4}	8.3×10^{-5}	40.0	0.40	38.5	45	0.00280
6	1.67×10^{-4}	2.5×10^{-4}	28.0	0.86	26.0	55	0.00373
7	1.67×10^{-4}	3.3×10^{-4}	22.0	0.90	19.0	54	0.00659
8	3.3×10^{-4}	8.3×10^{-5}	44.5	0.45	40.0	28	0.00305
9	3.3×10^{-4}	1.67×10^{-4}	24.5	0.50	21.0	60	0.00518
10	3.3×10^{-4}	2.5×10^{-4}	32.0	0.97	26.0	42	0.00410
11	5.0×10^{-4}	8.3×10^{-5}	41.0	0.40	39.0	24	0.00268
12	5.0×10^{-4}	1.67×10^{-4}	39.5	0.80	38.0	64	0.00312
13	5.0×10^{-4}	2.5×10^{-4}	27.0	0.82	26.0	65	0.00388
14	5.0×10^{-4}	3.3×10^{-4}	22.0	0.90	20.5	82	0.00491
15	6.67×10^{-4}	8.3×10^{-5}	35.0	0.36	33.0	46	0.00360
16	6.67×10^{-4}	1.67×10^{-4}	23.5	0.48	23.0	74	0.00515
17	6.67×10^{-4}	2.5×10^{-4}	26.0	0.80	24.0	72	0.00437
18	6.67×10^{-4}	3.3×10^{-4}	21.0	0.86	19.5	95	0.00498

Table 4. Holdup and Peclet number for extrudates.

Run No.	Q_g (m^3/s)	Q_1 (m^3/s)	$\bar{t}$ (s)	H_T	$\bar{t}_m$ (s)	Pe	1/n Σ|Y(t)–Y_m(t)|
1	0	8.3×10^{-5}	35.0	0.35	34.0	30	0.00281
2	0	1.67×10^{-4}	29.5	0.60	27.5	22	0.00362
3	0	2.5×10^{-4}	28.5	0.87	27.0	23	0.00451
4	0	3.3×10^{-4}	23.5	0.95	22.0	38	0.00308
5	1.67×10^{-4}	8.3×10^{-5}	42.5	0.43	42.0	29	0.00303
6	1.67×10^{-4}	1.67×10^{-4}	34.0	0.68	32.0	19	0.00295
7	1.67×10^{-4}	3.3×10^{-4}	23.0	0.95	23.0	40	0.00573
8	5.0×10^{-4}	8.3×10^{-5}	34.0	0.35	34.0	58	0.00331
9	5.0×10^{-4}	1.67×10^{-4}	28.5	0.59	27.0	30	0.00356
10	5.0×10^{-4}	2.5×10^{-4}	27.5	0.84	26.0	32	0.00316
11	5.0×10^{-4}	3.3×10^{-4}	24.0	0.96	23.0	28	0.00313
12	6.67×10^{-4}	8.3×10^{-5}	42.0	0.36	41.0	30	0.00251
13	6.67×10^{-4}	1.67×10^{-4}	33.0	0.52	30.5	26	0.00354
14	6.67×10^{-4}	2.5×10^{-4}	31.5	0.95	30.0	22	0.00481
15	6.67×10^{-4}	3.3×10^{-4}	24.0	0.98	23.0	34	0.00828

$$(7) \quad \frac{\partial C}{\partial \theta} = \frac{1}{Pe}\frac{\partial^2 C}{\partial X^2} - \frac{\partial C}{\partial X}$$

where: C – dimensionless tracer concentration = c(t)/c(0), Pe – Peclet number = ul/D, X – dimensionless axial co-ordinate = x/L, u – mean linear velocity, D – axial dispersion coefficient, c(t) – tracer concentration at time t, c(0) – initial concentration.

The solution of the above equation for open-open boundary condition of equation in dimensionless form is given as [2, 5]

$$(8) \quad E(\theta) = \sqrt{\frac{Pe}{4\pi\theta}} \exp. \frac{-Pe(1-\theta)^2}{4\theta}$$

The MRT and variance of impulse characterstics, E(q) are given by the following relations:

$$(9) \quad \bar{t} = \left(1 + \frac{2}{Pe}\right)\tau$$

$$(10) \quad \frac{\sigma^2(t)}{\bar{t}^2} = \frac{2}{Pe} - \frac{8}{Pe^2}$$

The response of a system to an ideal impulse directly gives RTD of fluid flowing in the system, which is directly compared with the model RTD. However, it is not always practically feasible to inject tracer as an ideal impulse and in such situations the tracer is injected as a pulse. The model response, $Y_m(t)$ of a linear system to an arbitrary pulse of tracer is obtained by convoluting the input function, X(t) with impulse response of the model, E(t). Thus [4, 5].

$$(11) \quad Y_m(t) = \int_0^t X(t-T)\, E(t)\, dT$$

For discrete time interval, the above convolution integral can be written as:

$$(12) \quad Y_m(t) = \sum_0^t X(t-T)\, E(t)\, \Delta T$$

One of the oldest and simplest techniques of parameter estimation is the moment's method, which involves the comparison of variances of the model and experimental distribution functions. Unfortunately there are some inherent computational errors involved in the variance of the measured response curves. The variance is computed from the first and second moments about the origin of the experimentally measured tracer concentration distribution curve. In the

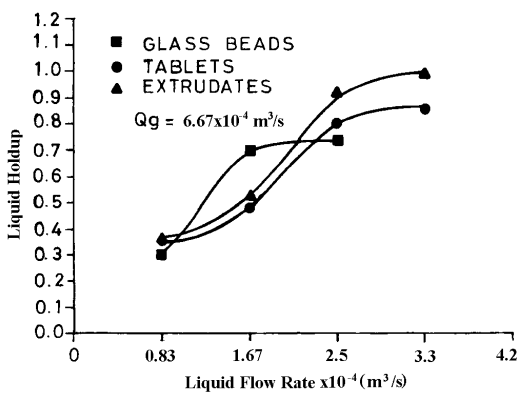

Fig. 3. Comparison of liquid holdup as a function of liquid flow rate for different packings.

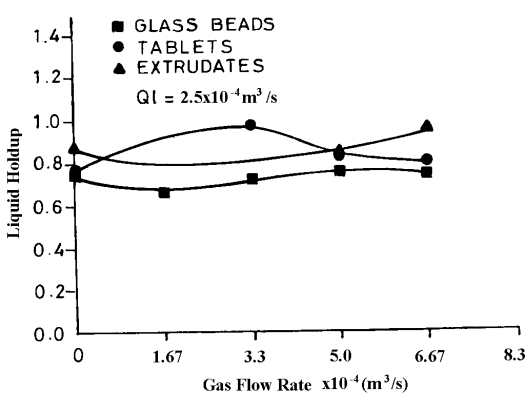

Fig. 4. Comparison of liquid holdup as a function of gas flow rate for different packings.

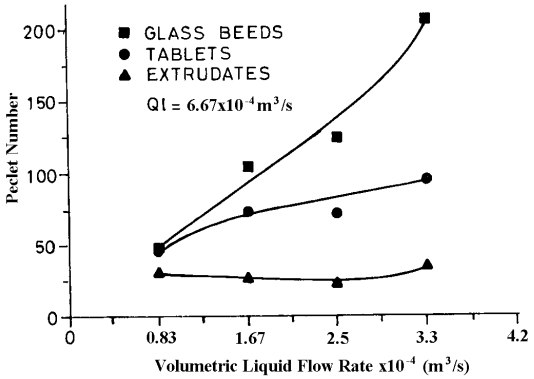

Fig. 5. Comparison of Peclet number as a function of liquid flow rate for different packings.

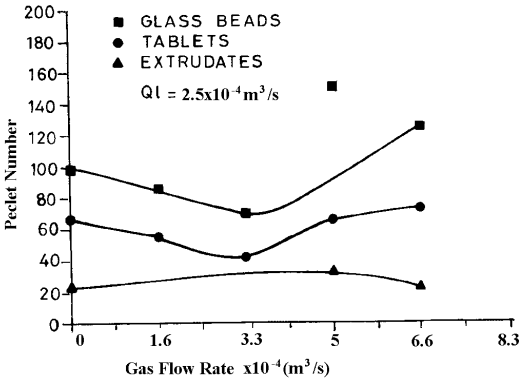

Fig. 6. Comparison of Peclet number as a function of gas flow rate for different packings.

estimation of moments, the values of concentration c(t) at large time (t) are weighed heavily. The weighing factor consists of t for the first moment and t^2 for the second moment. Since the 'tail' of a tracer response curve is the least precisely recorded portion due to the small value of concentration involved, the computed moments will have a large error. In addition to the above disadvantage, the method assumes that the model is an exact description of the flow system and no check of model applicability is provided. The values of model parameter estimated by the moment method can be considered only as a rough estimate.

The disadvantage of the moment method could be avoided by fitting the complete model RTD curve with the experimental RTD curve. The least–squares curve-fitting method using the well-known Marquardt-Levenberg algorithm is used to fit the two curves and obtain the optimum model parameters. The quality of the fit is judged by choosing the model parameters to minimise the sum of the squares of the differences between the experimental and model computed curves [6]. The values of the model parameters (MRT and Pe) corresponding to the minimum value of root mean square error (RMS) or absolute deviation error (ADE) are chosen as the optimum values. Thus:

$$(13)\quad \mathrm{RMS} = \left\{ \frac{1}{n} \sum \left| Y(t) - Y_m(t,\ \text{parameters}) \right|^2 \right\}^{0.5} = \text{Minimum}$$

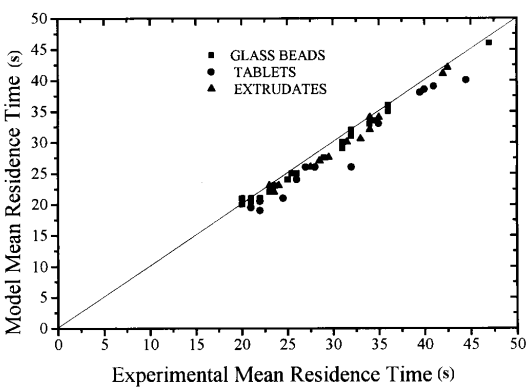

Fig. 7. Comparison of experimental and model MRTs.

or

$$(14)\quad \mathrm{ADE} = \frac{1}{n} \sum \left| Y(t) - Y_m(t,\ \text{parameters}) \right| = \text{Minimum}$$

The three representative plots of model simulation for glass beads, tablets and extrudates are shown in Figs. 2a, 2b and 2c, respectively. The values of MRT ($\bar{t}_m$) and Peclet number obtained by model simulation, at different operating conditions used, are given in Tables 2, 3 and 4 for glass beads, tablets and extrudates, respectively.

Results and discussion

The tracer concentration distributions recorded by detector D_2 and D_3 were compared to analyse the radial distribution of liquid phase in the column. Efficiencies were so adjusted that both the detectors have the same response. The superimposition of tracer distribution curves recorded in different runs indicated no significant radial maldistribution and is thus neglected because of small diameter to length ratio of the reactor.

It can be observed that liquid holdup increases with increase in liquid flow rate for all the three types of packings. One of the representative plots of liquid hold up *vs.* liquid flow rate is shown in Fig. 3. The liquid holdup is found to be independent of the gas flow rate. Fig. 4 shows the variation in holdup with gas flow rate for three different types of packing.

It is observed that Pe increases with increase in liquid flow rate in general for glass beads and tablets. For extrudates it is almost constant. A representative plot of variation of Pe with liquid flow rates is shown in Fig. 5. No specific trend in Pe with varying gas flow rate has been observed. One of the plots showing the variation in Pe with gas flow rates for glass beads, tablets and extrudates is shown in Fig. 6. The values of Pe for glass beads are higher than the corresponding values for tablets and extrudates. The values of Pe with tablets are higher than that for extrudates as can be seen in Fig. 6. The values of MRT estimated by model simulation are almost same as experimentally measured values. A comparison of the two is shown in Fig. 7.

Conclusions

From this study the following conclusions have been drawn:

1) No significant radial maldistribution was observed.

2) The liquid holdup increases with increase in liquid flow rate and is almost independent of gas flow rate used in the study for all the packings.

3) For glass beads and tablets the axial dispersion (D) of liquid phase decreases with increasing liquid flow rate and is constant for extrudates. However, no specific trend in axial dispersion (D) is observed with respect to varying gas flow rates.

4) The model estimated MRTs are in good agreement with MRTs measured experimentally. This justifies that the axial dispersion model is suitable to describe the dynamics of liquid phase in TBRs filled with non-porous catalyst particles.

5) The liquid holdup and degree of axial dispersion of liquid (Pe) are strongly dependent upon shape and size of the catalyst used in TBRs. The degree of axial dispersion is less with spherical catalyst than the catalyst of tablet and extrudate shapes.

6) The results obtained in this study will be useful for scale-up, design and to optimise the performance of full scale industrial TBRs.

7) Radiotracer techniques provide an excellent tool to study the holdup and degree of axial mixing of flowing media in TBRs.

Acknowledgments Authors are grateful to Dr. S.M. Rao and Dr. S.V. Navada for their help and support during the course of this work.

References

1. Danckwerts PV (1953) Continuous flow systems, distribution of residence times. Chem Eng Sci 2:1–13
2. Fu Meng Shyang, Chung-Shung Tan (1996) Liquid holdup and axial dispersion in trickle bed reactors. Chem Eng Sci 51:5357–5361
3. Gianetto A, Specchia V (1992) Trickle bed reactors: state of art and perspectives. Chem Eng Sci 47:3197–3213
4. Guidebook on radioisotope tracers in industry (1990) Technical Report Series No. 316. IAEA, Vienna
5. Levenspiel O (1996) Chemical reaction engineering. 2nd edn. Wiley, New York
6. Michelsen ML (1972) A least-squares method for residence time distribution analysis. Chem Eng J 4:171–179
7. Residence Time Distribution software analysis (1996) Computer Manual Series No. 11. IAEA, Vienna
8. Saroha AK, Nigam KDP (1996) Trickle bed reactors. Reviews in Chemical Engineering 12:207–347
9. Saroha AK (1997) Studies on multiphase reactors. Ph.D. Thesis, Indian Institute of Technology, Delhi, India